



# Fabrication of TiO<sub>2</sub> Nanoflowers Powder with Various Concentration of CTAB

S. Shamsudin<sup>1</sup>, M.K. Ahmad<sup>1, \*</sup>, N. Nafarizal<sup>1</sup>, C.F. Soon<sup>1</sup>, R.A. Rahim<sup>2</sup>,  
D. A/L Alakendram<sup>2</sup>, M. Shimomura<sup>3</sup> and K. Murakami<sup>3</sup>

<sup>1</sup>Microelectronic and Nanotechnology-Shamsuddin Research Centre (MiNT-SRC) Faculty of Electrical and Electronic Engineering, Universiti Tun Hussein Onn Malaysia, Parit Raja, Batu Pahat, Johor, MALAYSIA

<sup>2</sup>Department of Science Faculty of Electrical and Electronic Engineering, Universiti Tun Hussein Onn Malaysia, 86400 Parit Raja, Batu Pahat, Johor, MALAYSIA

<sup>3</sup>Department of Engineering, Graduate School of Integrated Science and Technology, Shizuoka University, 432-8011 Hamamatsu, Shizuoka, JAPAN

\*Corresponding Author

DOI: <https://doi.org/10.30880/ijie.2020.12.02.023>

Received 29 December 2019; Accepted 27 January 2020; Available online 28 February 2020

**Abstract:** Nanostructures titanium dioxide (TiO<sub>2</sub>) such as nanoflowers and nanorods have contribute in many application. Among TiO<sub>2</sub> nanostructures, TiO<sub>2</sub> nanoflowers gives high surface area that contribute in good binding properties and reducing internal stress and increasing strength of the ceramics. This paper presents fabrication of TiO<sub>2</sub> nanoflowers powder to overcome the cracking problem in ceramic industry. In this study, fabricated rutile-phased TiO<sub>2</sub> nanoflower powder has been successfully synthesized by using hydrothermal method and the surface morphology, structural properties, and the composition of TiO<sub>2</sub> nanoflower powder also identified. The fabricated TiO<sub>2</sub> are characterized using Field Emission Scanning Electron Microscopy (FESEM) to observe the surface morphology of TiO<sub>2</sub>, X-ray Dispersion (XRD) was used to determine the crystallite phase and EDX for element composition in fabricated TiO<sub>2</sub> powder. The synthesized TiO<sub>2</sub> powder was obtained from the reaction between deionized water (DI), hydrochloric acid (HCl), Titanium Butoxide (TBOT) and Cetyltrimethylammonium Bromide (CTAB). The hydrothermal temperature is 150 C with fixed hydrothermal time of 10 hours. The parameters varied is the mass of surfactant used, CTAB. The hydrothermal method is proven suitable to fabricate semiconductor materials due to its advantages that parameters are easily modified and can be performed under closed system with low operational temperature. Increased amount of CTAB used make the gap between the nanorod become closer and stronger. The diffraction peaks of all sample hardly changed, but the intensity for each sample was enhanced as the mass of CTAB used increased. The structure also become well crystallined in rutile phase structure.

**Keywords:** Ceramics, hydrothermal, nanoflowers, surfactant. TiO<sub>2</sub> powder

## 1. Introduction

The invention atmospheric pressure plasma has become very popular nowadays due to its wide promising applications, especially in the biomedical field (C.F. Goodeve *et al.*, 1983; F. Kato *et al.*, 1956). This low temperature

\*Corresponding author: [akhairul@uthm.edu.my](mailto:akhairul@uthm.edu.my)

and simple system open up new possibility in sterilization, inactivation of a cancer cell, wound healing and tooth bleaching (A. Fujishima *et al.*, 1972; S.N. Frank *et al.*, 1977; D. Gopi *et al.*, 2012). The advantage of plasma sterilization can be a great benefit in the industries of food preparation, health care, engineering production and more. Plasma sterilization is a process to remove micro-organism and contamination. The high rate of efficiency or total removal of the micro-organism is needed to make sure the treated surface is safe to be used (N. Aman and T. Mishra, 2013). In current technology, there are variety of sterilization process in order to achieve the highest removal of bacteria such as moist and dry heat sterilization, chemical sterilization, irradiation and gas plasma sterilization (M.C Wu *et al.*, 2011). The ideal of sterilization process has been discussed by Moisen *et. al.* that the process should have short times of sterilization, low temperature of the process and provide safety encounter to people and the environment (A.L. Linsebigler *et al.*, 1995). However, a deep understanding of plasma sterilization fundamental is needed in the process to develop functional plasma sterilization from research into reality market. Thus, this study reveals the efficiency evaluation of the APPNJ to deactivate E-coli as one of tough and dormant bacteria.

Each phase of  $\text{TiO}_2$  has different crystalline structure but still expressed in the same chemical formula of  $\text{TiO}_2$ . Usually,  $\text{TiO}_2$  is applied for cosmetic, medicine, paints and food industries in white solid powder forms. The stability of  $\text{TiO}_2$  phases depends on the size. It was proven that rutile is the most stable when its particle size above 35 nm while anatase and brookite become stable when their particle size lower than 11 nm and between the range 11-35 nm respectively (T. Luttrell *et al.*, 2014). The anatase phase structure formed at a temperature lower than 450 while rutile will only appear at a higher temperature which is 600 and above (D.A.H. Hanaor and C.C. Sorrell, 2011; D.O. Scanlon *et al.*, 2013; S. Rehman *et al.*, 2009). For better understanding, Figure 1 illustrates the structure and image of each polymorph.

Hydrothermal method is a promising method to obtain nanocrystalline titania particles. The hydrothermal process in which the chemical reaction could take place under auto-generated pressure upon heating is efficient to achieve crystalline phase at relatively low temperature. Hydrothermal processing of materials is a technology that is preferred today due to its advantages of easy to be prepared and low cost (P. Calza *et al.*, 1997; A.L. Linsebigler *et al.*, 1997; A. Fujishima *et al.*, 2000; A. Fujishima *et al.*, 2008). Titanium dioxide can be obtained by using the hydrothermal synthesis. A chemical reaction takes place under auto-generated pressure during heating. This process which happens during the hydrothermal process at low temperature is essential to obtain the crystalline phase. Preparation of  $\text{TiO}_2$  using hydrothermal method take place in a closed system which makes it environmentally friendly. Under the hydrothermal condition, some properties of nanoflower such as phase, particle size and crystallinity can be controlled. The obtained results from the hydrothermal method are expected to have large surface area, smaller crystalline size and higher stability than other conventional methods.

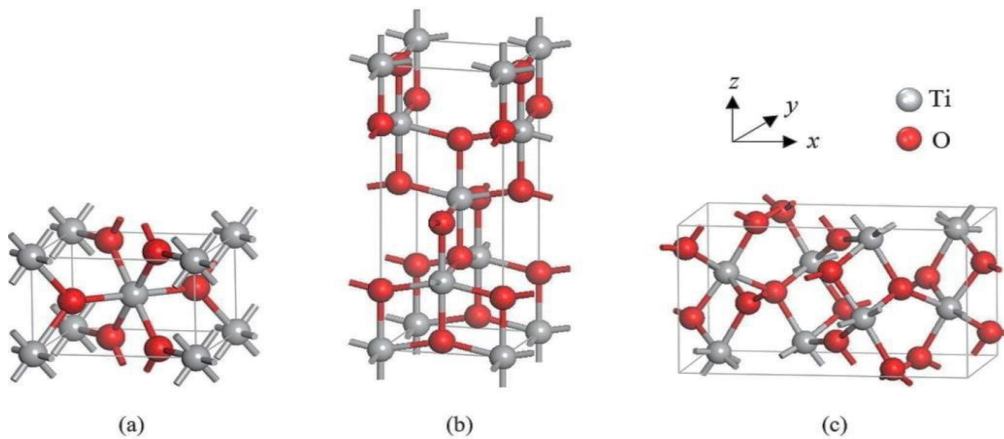


**Fig. 1 - The primitive unit cell of (a) rutile, (b) anatase and (c) brookite  $\text{TiO}_2$  (M.H Samat *et al.*, 2016)**

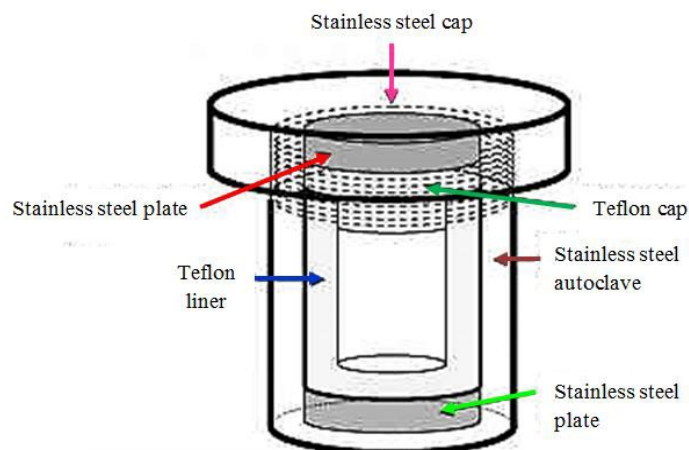


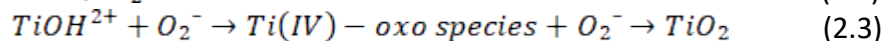
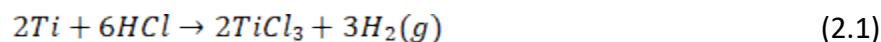
Fig. 2 - Schematic diagram of autoclave

## 2. Experiment

### 2.1 Preparation of TiO<sub>2</sub> Nanoflower Powder

The nanostructured TiO<sub>2</sub> powder had been prepared by using the hydrothermal method at 150°C for 10 hours. The deionized water (DI), hydrochloric acid (HCL) and titanium (IV) butoxide (TBOT) were mixed and used as precursor solution and the cetyltrimethylammonium bromide (CTAB) act as surfactant for the in precursor solution. The parameter that was varied in this study is the mass of CTAB which is 0.5g, 1.0g, 1.5g, 2.0g and 2.5g and another sample is commercial TiO<sub>2</sub> powder which is Degussa P25 TiO<sub>2</sub> powder which will be used without any purification and labeled as sample 6 in this experiment. There are five steps to fulfill the aim of this study which is the glass cleaning, hydrothermal process, grinding, annealing process and characterization. Firstly, the glass immersed in cleaning solution and cleaned using the ultrasonic cleaner for 10 minutes. Figure 3 below show the flowchart for claeaning process of glass. The glass substrate was cleaned using acetone, ethanol and deionized water in an ultrasonic cleaner for about 10 minutes with the heat off. First, the substrates are washed using deionized water before placed on the cleaned beaker. Then the acetone is poured until the substrate is immersed. After that, the substrates undergo a cleaning process using an ultrasonic cleaner. After cleaned using acetone, the glass substrate is rinsed with deionized water. The process repeated using ethanol and lastly using deionized water.

The experiment starts with pouring 80 mL of deionized water into a beaker that placed on top of a magnetic stirrer. The stirrer was put into the beaker and the motion is set while the heat is off. After the deionized water stirrer for 10 minutes, 80 ml of hydrochloric acid, HCl was poured into the beaker that contained deionized water. The solution was stirred for 30 minutes. Then, 5 mL of titanium butoxide, TBOT was drop wisely into the mixed solution and left for a while until the precursor solution becomes clear and mixed well. Then, 0.5 g of CTAB was added to the precursor solution. After that, the glass substrates were put onto the Teflon-lined autoclave and the stock solution was poured wisely into the Teflon. Then, the autoclave containing substrates and stock solution is put in the oven for hydrothermal reaction. The reaction was set at a fixed temperature of 150 for 10 hours. In order to study the effect of surfactant CTAB, the experiment was repeated with a different mass of CTAB which is 1.0 g, 1.5 g, 2.0 g, and 2.5 g. After the hydrothermal reaction, the autoclave is placed at room temperature to cool down. The hydrothermal reaction occurred inside the autoclave can be explain by using equation (2.1) - (2.3):



Then, the substrate is cleaned using deionized water before left to dry in the oven under 60 °C for 5 minutes. Then, the synthesized TiO<sub>2</sub> powder was take out from the glass substrate and grinded with a pestle. Then the annealing process take place for 30 minutes with temperature 500 °C. Table 1 shows the number of samples prepared and ratio of chemicals used.

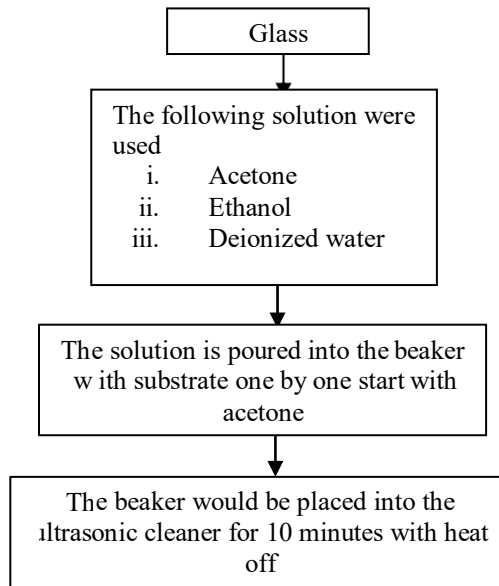


**Fig. 3 - Substrate cleaning process**

**Table 1- Sample prepared and chemical ratio**

Sample	Chemicals ratio
1	80 ml DI : 80 ml HCl : 5 ml TBOT : 0.5 g CTAB
2	80 ml DI : 80 ml HCl : 5 ml TBOT : 1.0 g CTAB
3	80 ml DI : 80 ml HCl : 5 ml TBOT : 1.5 g CTAB
4	80 ml DI : 80 ml HCl : 5 ml TBOT : 2.0 g CTAB
5	80 ml DI : 80 ml HCl : 5 ml TBOT : 2.5 g CTAB
6	Degussa P25

## 2.2 Characterizations

The investigation on final obtained nanostructured was characterized by using a Field-Emission Scanning Electron Microscope (FE-SEM, JEOL, model JSM-7600F) for its surface morphology (A. Alyamani and O. Lemine, 2012). The structural analysis of the samples was carried out using X-Ray Diffraction (XRD), RAMAN spectroscopy used to analyze the intensity while element involved in sample were characterized using EDX.

## 3. Result

### 3.1 Morphological Properties of TiO<sub>2</sub> Nanostructures

The Field Emission Scanning Electron Microscopy (FESEM) is used to observe the surface morphology of the prepared rutile phase TiO<sub>2</sub> powder. The FESEM has higher resolution, so that samples can be magnified at higher level. From the figure below shows the analysis of FESEM images x25000 magnifications. Figure 4 (a) to (e) shows the FESEM images of the TiO<sub>2</sub> powders prepared by hydrothermal method at various mass of CTAB. While Figure 4 (f) indicates the FESEM image of the commercial TiO<sub>2</sub> powder that observed directly without any treatment. From the observation of Figure 4 (f), the nanoparticles seem agglomerates and in anatase phase while morphologies in Figure 4 (a) until (e), the particles slowly become less agglomerates. The sample in Figure 4 (f) was observed to make a comparison between commercial Degussa P25 TiO<sub>2</sub> powder and synthesized TiO<sub>2</sub> powder. It can be observed that CTAB act as a surfactant to control the formation of TiO<sub>2</sub> nanostructured that help to make it less agglomerates (C.A. Ruslimie *et al.*, 2010; Y. Kajita *et al.*, 2012).

It was observed that the morphologies and size of prepared samples are greatly depend on the conditions of synthesis. Furthermore, the acidity of the used solution determined the final crystal structure of the formed particles. When acid content was very high, the structure of the powder sample become rutile. FESEM patterns showed in Figure 4 (a)-(e) indicates the changes of TiO<sub>2</sub> nanostructures with the formation of TiO<sub>2</sub> nanoflower. The morphologies shown in Figure 4 (a)-(e) is random TiO<sub>2</sub> nanocrystals aggregations that obtained with presence of 0.5, 1.0, 1.5, 2.0, and 2.5 g of CTAB.

The microspheres comprised of nanorods start to form after hydrothermal process can be seen under higher FESEM magnification. The structure composed of large quantities of elongated crystal nanorods which are closely packed with square profiles that radially aligned is successfully fabricated. The microspheres were formed by radial growth of nano-acicular crystal on the TiO<sub>2</sub> nanoparticulate core. In these samples, the rough surface of TiO<sub>2</sub> microspheres was observed. When the mass of CTAB used increase, the hydrolysis rate is decreased and then the size of nanoflower decrease while the surface area increase. Cationic surfactant CTAB modifying rutile TiO<sub>2</sub> during its formation from hydrolyzed TBOT in solution. The hydrolysis rate of TBOT in hydrothermal process resulting the formation of rutile phase TiO<sub>2</sub> powder. Presence of CTAB make the nanorods become more densely packed due to smaller clusters consisting of near-spherical particles and this suggesting an increase in the effective surface area. Bridged OH groups are expected to be acidic in character, owing to their strong polarization by Ti(IV). Thus, the hydrogen atoms of bridged OH groups of titanium(IV) oxo species are exchangeable with cationic headgroups of CTAB (I.K Konstantinou *et al.*, 2004; M.R. Hoffmann *et al.*, 1995). Thus, it was observed that the morphologies and size of prepared samples are greatly depends on its synthesis condition.

The microspheres comprised of nanorods start to grow after hydrothermal process and it can be seen from higher FESEM magnification that the structure composed of large quantities of elongated crystal nanorods which are closely packed with square profiles that radially aligned. The microspheres were formed by radial growth of nano-acicular crystal on the TiO<sub>2</sub> nanoparticulate core. In these samples, the rough surface of TiO<sub>2</sub> microspheres was observed (J.P. Nikkanen *et al.*, 2007).

TiO<sub>2</sub> nanoflowers powder was mixed with raw material of ceramics to give better in binding property. No similar product in the market that has such morphology and structure. The space and gap between each particles is get stronger and closer when the amount of CTAB is increase. The shape of the nanoflowers become more clear and sharp at the edge of particles to increase the efficiency with increment in CTAB amounts.

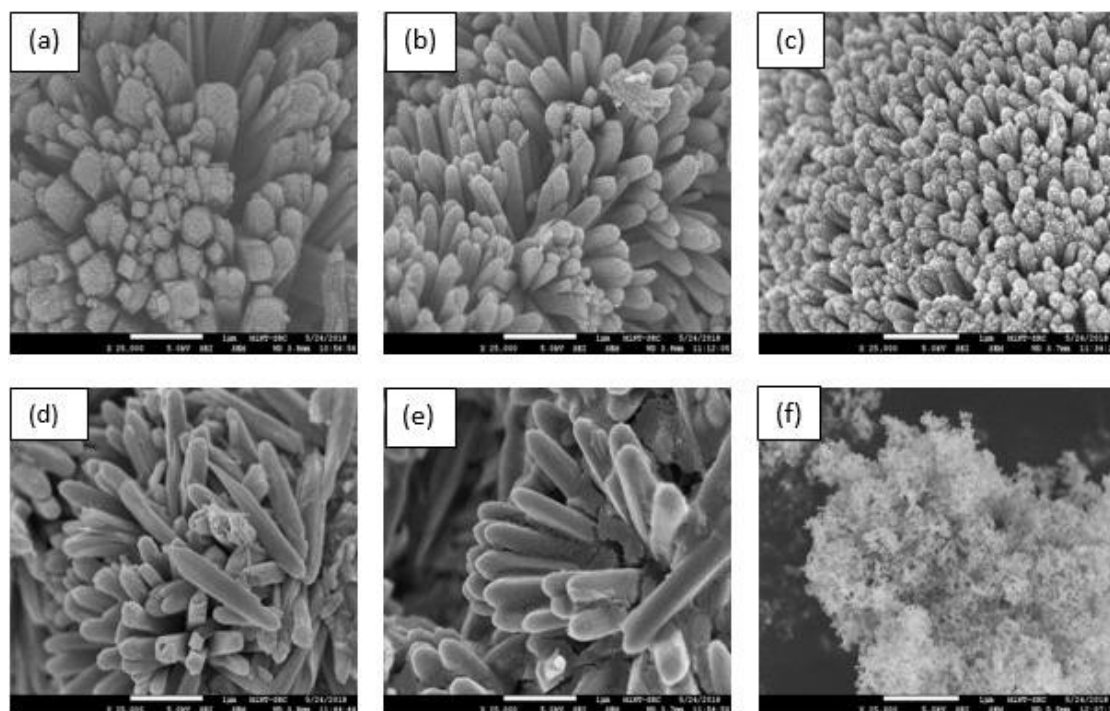


Fig. 4 - FESEM image under X25000 magnification for (a) 0.5 g CTAB, (b) 1.0 g CTAB, (c) 1.5 g CTAB, (d) 2.0 g CTAB, (e) 2.5 g CTAB and (f) P25.

### 3.2 Crystalline structure of TiO<sub>2</sub> Nanoflower powder

The x-ray diffraction pattern of the synthesized titanium nanoparticles is shown in Figure 5. The x-ray diffraction data analysis was carried out by using x-ray powder diffraction model. The degree of crystallinity and the crystal structure are characterized by using x-ray diffraction (XRD). The peak pattern shows from the XRD result indicates the phase transformation as the sample were varied for mass of CTAB. From Figure 5, it show clearly that all the sample represents rutile phase. The prepared sample TiO<sub>2</sub> have the same crystal structure of the rutile phase with tetragonal crystal structure despite of their different morphologies which is shown in Figure 4. The rutile phase of TiO<sub>2</sub> was analysed at diffraction peaks (110), (111), (211), (220), (310) and (301) rutile phase diffraction planes relatively. XRD results indicates that the TiO<sub>2</sub> powder were pure rutile as shown by the diffraction planes. The peaks were referred to pdf number 00-021-1276 for standard diffraction data of rutile. The shape of diffraction peaks suggest that the products are well crystallized. When the mass of CTAB used increase, the diffraction peaks of rutile TiO<sub>2</sub> phase with different morphologies hardly change, but their intensity is enhanced, which is confirmed by the height and width of the diffraction peaks (T. Sreethawong *et al.*, 2012) The (110) and (111) have different morphologies of TiO<sub>2</sub> powder and the growth direction of TiO<sub>2</sub> nanorods is concluded to be parallel to (110) diffraction plane and corresponding to the tetragonal rutile phase of TiO<sub>2</sub> nanorods. The intensity of XRD peaks of the sample reflects that the formed nanoparticles are crystalline and broad diffraction peaks indicate very small size crystallite. The efficiency is increases with increasing the amount of CTAB used.

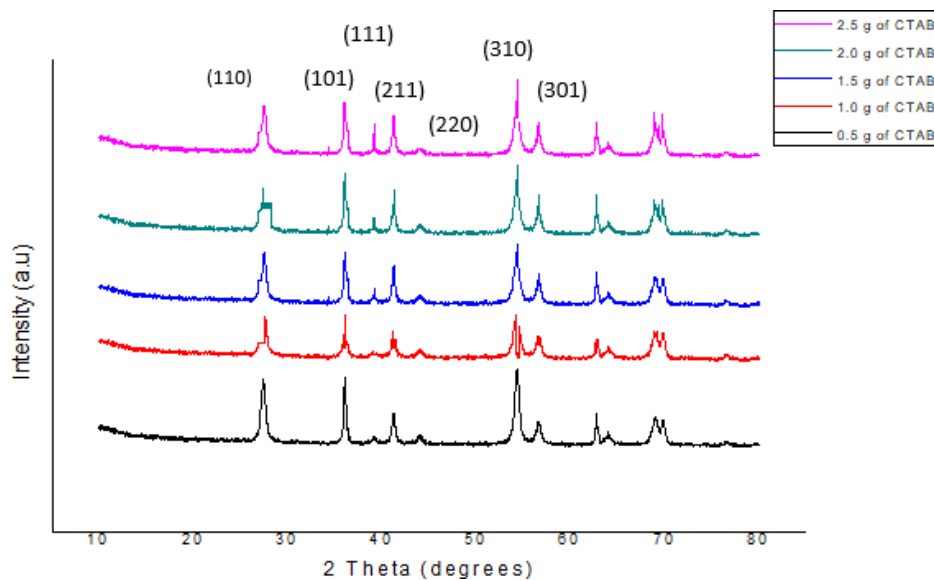


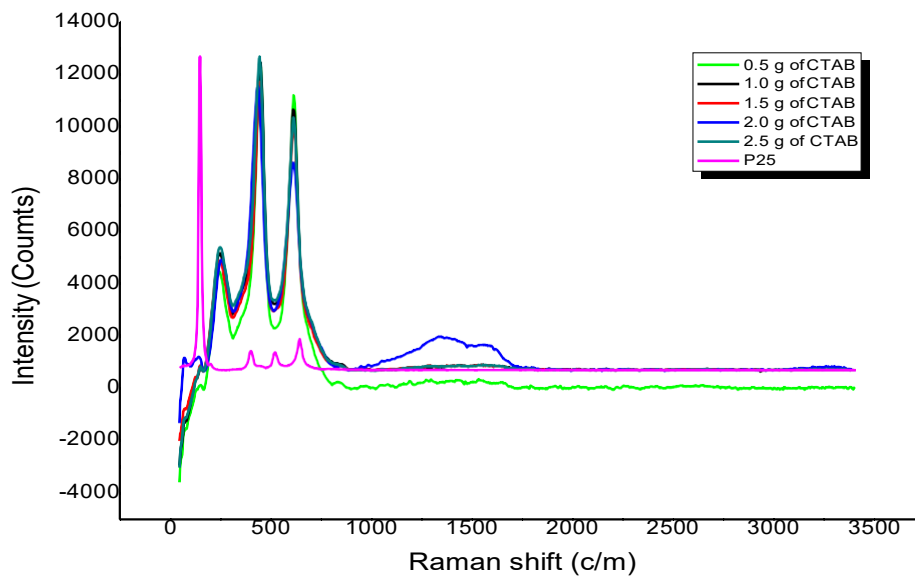
Fig. 5- XRD patterns for TiO<sub>2</sub> sample with 0.5 g, 1.0 g, 1.5 g, 2.0 g and 2.5

### 3.3 RAMAN of TiO<sub>2</sub> Nanoflower powder

Figure 6 shows Raman spectroscopy spectra of the various samples. There are three main Raman peaks characteristics of TiO were observed clearly. A sharp and large Raman peak is observed at 500 cm<sup>-1</sup> and additionally a small peak located at 1300 cm<sup>-1</sup>. As a result, no small peak has been formed. Hence, several factors such as phonon confinement, strain, non-homogeneity of the particle size distribution, defects and nonstoichiometry can contribute to the changes in the peak position, linewidth and shape of the Raman mode in rutile TiO<sub>2</sub> nanopowders. However, the separation between these various contributions is not straightforward. Dominance of one or more of these factors, observable in the Raman spectra, is determined by the structural characteristics of a TiO<sub>2</sub> nanopowder grain size and grain size distribution and existence of mixed phases anatase in combination with considerable amount of rutile or brookite phase. The Raman peaks characteristics of TiO<sub>2</sub> were observed clearly at 500cm<sup>-1</sup> and 1300cm<sup>-1</sup> for samples modes of the rutile phase.

**Table 2 - RAMAN Shift**

Amount of CTAB	p= peak position	a =peak height	W= FWHM	ar= peak area
0.5	1297.579	345.619	142.768	63892.5
1.0	1308.502	152.976	164.615	32521.97
1.5	1326.638	187.025	214.952	51588.51
2.0	1343.896	1352.025	335.017	573038
2.5	1534.36	203.104	288.564	74673.46
Degussa P25	645.597	1251.275	35.539	58191.18

**Fig. 6 - Raman spectroscopy spectra of the various samples**

### 3.4 EDX analysis of TiO<sub>2</sub> Nanoflower powder

The Energy Dispersive X-ray Spectroscopy (EDX) used to observe a structural morphology of the prepared rutile phase TiO<sub>2</sub> powder. It is powerful technique used to identify the elemental composition of as little as a cubic micron of material. The equipment is attached to the FESEM to allow for elemental information to be gathered about the specimen under investigation. The structural morphology of the prepared rutile phase TiO<sub>2</sub> with different CTAB weight are shown in Figures 7. The EDX result shows the atomic percentage of titanium is increasing while the atomic percentage of oxygen decreasing. It show that Titanium is as solid as steel however substantially less thick. All the samples show high purity with presence of Titanium and oxygen as the main elements. The characterization by using EDX only to show the presence of elements that involved in the formation of sample to support the data obtained in FESEM and XRD.

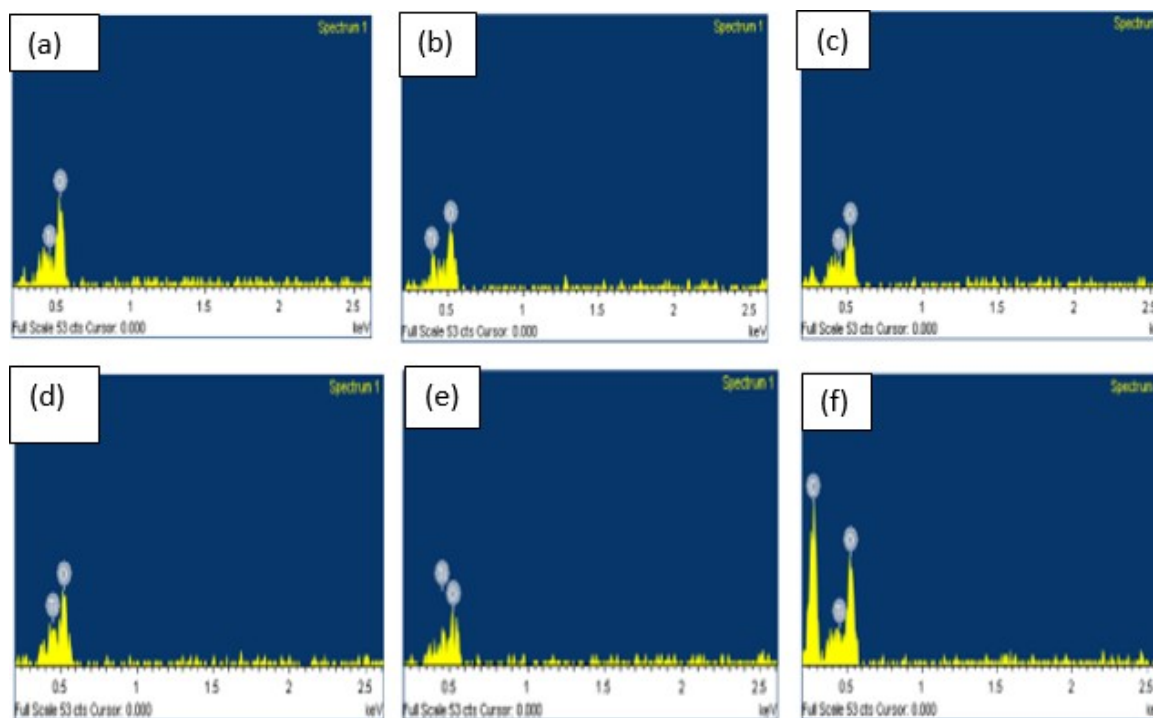


**Fig. 7- EDX data; (a) 0.5 g CTAB, (b) 1.0 g CTAB, (c) 1.5 g CTAB, (d) 2.0 g CTAB, (e) 2.5 g CTAB, and (f) Degussa P25.**

#### 4. Conclusion

In summary, rutile-phased  $\text{TiO}_2$  powder have been successfully fabricated through hydrothermal synthesis. The data analysis conclude that when the amount of CTAB increase, the atomic percentage of titanium also increase. Thus, it will increase the efficiency of powder to prevent cracking problem in ceramic industry.

#### Acknowledgement

The authors would like to acknowledge Research Grant Schemes Tier 1 Vot U859 of Universiti Tun Hussein Onn Malaysia, Ministry of Higher Education Malaysia for financial support. Facilities used in this study are supported by MiNT-SRC, Universiti Tun Hussein Onn Malaysia and special thanks to all members Microelectronic and Nanotechnology Shamsuddin Research Centre (MiNT-SRC) for technical support.

#### References

- [1] Goodeve, C.F and Kitchener, J.A. (1983). The mechanism of photosensitisation by solids. *Trans. Faraday Soc.*, Volume 34, 902-908.
- [2] Kato, F. and Mashio, S. (1956). Autooxidation by  $\text{TiO}_2$  as a photocatalyst. *Abtr. B. Annu. Meet Chem. Soc. Japan*, 223.
- [3] Fujishima, A. and Honda, K. (1972). Electrochemical photocatalysis of water at a semiconductor electrode. *Nature*, Volume 238, Issue 5358, 37-38.
- [4] Frank, S.N. and Bard, A.J. (1977). Heterogeneous photocatalytic oxidation of cyanide ion in aqueous solutions at titanium dioxide powder. *J. Am. Chem. Soc.*, Volume 99, 303-304.
- [5] Gopi, D., Indira, J., Kavitha, L., Sikar, M. and Modali, U.K. (2012). Synthesis of hydroxyapatite nanoparticles by a ultrasonic assisted with mixed hollow sphere template method. *Spectrochimica Acta Part A*, 131.
- [6] Aman, N. and Mishra, T. (2013). Photocatalytic materials and surfaces for environmental cleanup-II. *Journal of Recent Development on titania based mixed oxide photocatalysts for environmental application under visible light*, 196.
- [7] Wu, M.C., Sapi, A., Avila, A., Szabo, M., Hiltunen, J., Huuhtanen, M., Toth, G., Kukovecz, A., Konya, Z., Keiski, R., Su, W.F., Jantunen, H. and Kordas, K. (2011). Enhanced photocatalytic activity of  $\text{TiO}_2$  Nanofibers and their flexible composite films: *Decomposition of organic dyes and efficient  $\text{H}_2$  generation from ethanol-water mixtures*, 360-369.

- [8] Linsebigler, A.L., Lu, G. and Yates, J.T. (1995). Photocatalysis in TiO<sub>2</sub> surfaces: principle, mechanisms and selected results. *Chemical reviews*, 95, 735-758.
- [9] Luttrell, T., Halpegamage, S., Tao, J., Kramer, A., Sutter, E. and Batzill, M. (2014). Why is anatase a better photocatalyst than rutile?- model studies, on epitaxial TiO<sub>2</sub> films. *Scientific reports*, 4.
- [10] Hanaor, D.A.H. and Sorrell, C.C. (2011). Review of anatase to rutile phase transformation. *Journal of Materials Science*, 46, 855-874.
- [11] Scanlon, D.O., Dunhill, C.W., Buckeridge, J., Shevlin, S.A., Logsdail, A.J., Woodley, S.M. Richard, C., Catlow, A., Powell, M.J., Palgrave, R.G., Parkin, I.P., Watson, G.W., Keal, T.W., Sherwood, P., Walsh, A., Sokol, A.A. (2013). Band alignment of rutile and anatase TiO<sub>2</sub>. *Nature Materials* 12, 798-801.
- [12] Rehman, S., Ullah, R., Butt, A.M. and Gohar N.D. (2009). Strategies of making TiO<sub>2</sub> AND ZnO visible light active. *J. Hazard Mater*, 170(2-3):560-569.
- [13] Albanis, C.A. Razali, M.H. and Khairul, W.M. (2010). Effect of HTAB concentration on the synthesis of nanostructured TiO<sub>2</sub> towards its catalytic activities. *The Malaysia Journal of Analytical Sciences*, Volume 14, Issue 1, 41-49.
- [14] Konstantinou, I.K. and Albanis, T.A. (2004). TiO<sub>2</sub> assisted photocatalytic degradation of azo dyes in aqueous solution: kinetic and mechanistic investigation- a review. *Appl. Catal. B: Environ*, 49, 1-14.
- [15] Hoffmann, M.R., Maartin, S.T., Choi, W. and Behenemann, D.W. (1995). Environmental application of semiconductor photocatalysis, *Chem. Rev.* 95, 69-96.
- [16] Samat, M.H., Ali, A.M.M., Taib, M.F.M., Hassan, O.H. and Yahya, M.Z.A. (2016). Hubbard U calculations on optical properties of 3D transition metal oxide TiO<sub>2</sub>. *Journal of Physics*, 891-896.
- [17] Calza, P., Minero, C. and Pelizzetti, E. (1997). Photo-catalytic assisted hydrolysis of chlorinated methane in the presence of electron and hole scavengers. *Environment Science Technologies*.
- [18] Linsebigler, A.L., Lu, G. and Yates, J.T. (1995). Photocatalysis in TiO<sub>2</sub> surfaces: principles, mechanisms & selected results. *Chemical reviews*, 95, 735-758.
- [19] Fujishima, A., Rao, T.N. and TRYK, D.A. (2000). Titanium dioxide photocatalysis. *Journal of photochemistry & photobiology: photochemistry reviews*, 1-21.
- [20] Fujishima, A., Zhang, X. and TRYK, D.A. (2008). TiO<sub>2</sub> photocatalysis and related surface phenomena. *Surface science reports*, 515-582
- [21] Alyamani, A. and Lemine, O. (2012). FE-SEM Characterization of some nanomaterial. *Intech*, 1, 463-472.
- [22] Ruslimie, C.A., Razali, M.H. and Khairul, W.M. (2010). Effect of HTAB Concentration On The Synthesis of TiO<sub>2</sub> Nanostructured Towards its Catalytic Activities. *The Malaysia Journal Of Analytical Sciences*, 14,41-49.
- [22] Kajita, Y., Pihosh, Y., Mawatari, K. and Kitamari, T. (2012). Development of Light-Driven H<sub>2</sub>/O<sub>2</sub> Generation Chip for Micro Fuel Cell Devices. 16<sup>th</sup> International Conference on Miniature Systems for Chemistry and Life Sciences, Okinawa, Japan.
- [23] Nikkanen, J.P., Kanerva, T. and Mantyla, T. (2007). The effect of acidity in low-temperature synthesis of titanium dioxide. *Journal of Crystal Growth* 304, 179-183.
- [24] Sreethawong, T., Ngamsinlapasathian, S and Yoshikawa, S. (2012). Surfactant-aided-sol-gel synthesis of mesoporous-assembled TiO<sub>2</sub> - NiO mixed oxide nanocrystals and their photocatalytic azo dye degradation activity. *Chemical Engineering Journal*, 292-300.